

Symmetry in halo displays and symmetry in halo-making crystals

Gunther P. Können

The relation between the symmetry in halo displays and crystal symmetry is investigated for halo displays that are generated by ensembles of crystals. It is found that, regardless of the symmetry of the constituent crystals, such displays are always left–right (L–R) symmetric if the crystals are formed from the surrounding vapor. L–R symmetry of a halo display implies here that the cross sections for formation of a halo arc on the left-hand side of the solar vertical and its right-hand side mirror image are equal. This property leaves room for two types of halo display only: a full symmetric one (*mmm*-symmetric), and a partial symmetric one (*mm2*-symmetric) in which halo constituents lack their counterparts on the other side of the parhelic circle. A partial symmetric display can occur only for point halos. Its occurrence implies that a number of symmetry elements are not present in the shape of the halo-making crystals. These elements are a center of inversion, any rotatory-inversion axis that is parallel to the crystal spin axis \mathbf{P} , a mirror plane perpendicular to the \mathbf{P} axis, and a twofold rotation axis perpendicular to the \mathbf{P} axis. A simple conceptual method is presented to reconstruct possible shapes of the halo-generating crystals from the halos in the display. The method is illustrated in two examples. Halos that may occur on the Saturnian satellite Titan are discussed. The possibilities for the Huygens probe to detect these halos during its descent through the Titan clouds in 2005 are detailed. © 2003 Optical Society of America

OCIS codes: 010.2940, 010.1290, 010.1110, 350.1270.

1. Introduction

This paper explores potentials and limitations of crystal determinations from halo observations. One motivation is the expanding number of photographically documented observations of halo arcs resulting from pyramidal ice crystals^{1,2} or perhaps from even more-exotic crystals.³ A second motivation is the possibility that the Huygens probe⁴ will detect halos resulting from exotic crystals during its descent in January 2005 through the atmosphere of the Saturnian satellite Titan.

The paper is divided into three parts. The first part, Section 2, discusses the relation between symmetry in halo displays and symmetry in halo-generating particles. The second part, Section 3, gives a recipe for crystal reconstruction from halo observations. The third part, Section 4, discusses potential Titan halos.

This paper can be regarded as an extension of the halo theory developed earlier⁵ to halos from crystal ensembles. In particular, Sections 2 and 3 here can be regarded as an elaboration of Sect. 3 of Ref. 5.

We consider refraction halos produced by preferentially oriented crystals. By refraction halos we mean halos that are due to refraction only. Any refraction halo arises from refraction by a wedge consisting of two faces of a crystal. However, we note that the conclusions about the relation between halo symmetry and crystal symmetry have a broader validity than for refraction halos alone.

We assume in this paper that gravity is the sole factor that determines the crystal orientation that will occur. We call this assumption the *Gravity Organizing Principle* (GOP). Among the situations that satisfy the GOP are crystals falling through still air or crystals floating at a fixed level in laminarily flowing air. Among the situations that do not satisfy the GOP are crystals that are subject to forces that are not parallel with the gravity vector \mathbf{G} or, in certain cases, crystals that are subject to torques. Examples of cases in which the GOP is not satisfied are crystals falling through a flow that has a vertical gradient in velocity; crystals floating in an undulating flow or in a flow that is forced around an object; crystals that are subject to electromagnetic forces;

G. P. Können (konnen@knmi.nl) is with the Royal Netherlands Meteorological Institute, P.O. Box 201, 3730AE De Bilt, The Netherlands.

Received 16 January 2002; revised manuscript received 13 May 2002.

0003-6935/03/030318-14\$15.00/0

© 2003 Optical Society of America

spinning crystals of certain shapes floating in a rotating flow; or, in certain cases, when non-Newtonian interactions are present between the crystals and the flow.

If the GOP is satisfied, then the aerodynamic conditions around a particle A spinning about a certain axis are identical to those around a particle B that is its mirror image with respect to a plane parallel to this axis and that is spinning with the same speed about this axis, but in the opposite direction.

Situations in nature in which the GOP is entirely fulfilled are rare. However, in most cases the forces acting on crystals causing the GOP to be dissatisfied are negligibly small. This implies that in practice the GOP often can be considered to be approximately satisfied.

The orientation of an airborne crystal that starts from some randomly chosen state will evolve toward a stable final state. This state can be random orientation or preferential orientation. If the GOP is satisfied and if the final state is not random orientation, then the orientations modes that can act as a final state to the crystal orientation and that can plausibly occur in reality will normally approximately satisfy the *Spin Vector Assumption* (SVA). The SVA, formulated in Ref. 5, Eq. (1) for individual wedges, implies that for any preferentially oriented crystal there is a unit vector \mathbf{P} (i.e., a spin vector) that is fixed in the crystal and has a constant zenith angle ψ . The crystal is otherwise unconstrained. Hence the crystal is free to rotate about the spin vector \mathbf{P} , and this vector is free to rotate about the vertical, represented by the zenith vector \mathbf{k} .

Reference 5 discusses halo displays from the standpoint of light scattering by an individual crystal. The orientation of the crystal is then preassigned in a mode that satisfies the SVA. It is automatically assumed that the crystal satisfies the SVA in the time domain. In considering ensembles of crystals, the SVA can be satisfied physically as in the single-crystal approach, or statistically. Satisfying the SVA physically in the entire ensemble assumes that all crystals are rotating about their \mathbf{P} and all \mathbf{P} s about the zenith. On the other extreme, satisfying the SVA statistically assumes that all crystals are fixed in space but with a distribution of their orientations that is the same as the distribution of the orientation in the time domain of a crystal that satisfies the SVA physically. Although these two extreme possibilities imply different aerodynamical conditions around the crystals, they result in identical halos. At places where the SVA is invoked in this paper, we assume that it is satisfied physically, being aerodynamically the more-complicated situation.

The shape of a refraction halo from a certain halo-making wedge follows uniquely from five parameters.⁵ These are the halo pole \mathbf{P}_u , which is the spin vector \mathbf{P} expressed in the wedge frame; the zenith angle ψ of \mathbf{P} ; the wedge angle α ; the solar elevation Σ , and the index of refraction n . The full halo display is obtained by considering ψ and n for any crystal in the

swarm, and then \mathbf{P}_u for any wedge that can be made up by the faces of any crystal.

As in Ref. 5, we consider only halos arising from spin axes vertically ($\psi = 0$) or horizontally ($\psi = 90^\circ$) oriented, giving rise to *point halos* and *great circle halos*, respectively. However, the symmetry properties for point halos discussed in Section 2 apply to other $\psi \neq 90^\circ$ halos also. As before⁵ we describe the halos by the *halo sphere*, which is a sphere on which each point represents a value of \mathbf{P}_u . The projection in the x direction of the halo sphere with dots on it representing the values of the halo poles \mathbf{P}_u is called a *pole diagram*. The halos discussed here can be generated by any substance, but to clarify the points raised we will often refer to examples from hexagonal ice crystals. Emphasis in the examples is on point halos.

2. Symmetry in Halo Displays

A. Symmetry Groups of Halos

Full halo symmetry arises if the halo poles for each wedge have *mmm*-symmetry—that is, if a halo pole $\mathbf{P}_u = (a, b, c)$ is accompanied by seven other poles, the full set having coordinates $(\pm a, \pm b, \pm c)$. For a given combination of $(n, \Sigma, \psi, \alpha)$ they need not be all non-empty; in other words, they need not all be capable of producing a halo. Also, in the generic case there are combinations of (n, α) in which no halo exists for any combination of $(\mathbf{P}_u, \Sigma, \psi)$, as in ice for $\alpha = 120^\circ$. Emptiness of halos may mask the full *mmm*-symmetry of a halo display. On the other hand, if full symmetry is present and all halos show up, then the display is left–right (L–R) symmetric with respect to the solar vertical while for $\psi = 0$ an upper arc (at $z > 0$ on the halo sphere) at either side is accompanied by another upper arc and two lower arcs ($z < 0$).

The lowest halo symmetry occurs when a halo with pole $\mathbf{P}_u = (a, b, c)$ is accompanied only by a halo with pole zrot $\mathbf{P}_u = (-a, -b, c)$ —which is the halo that occurs from face interchange of the wedge. The \mathbf{P}_u , zrot \mathbf{P}_u combination should always occur, although the two halos need not be simultaneously nonempty. In the generic case the shapes of these two halos are largely unrelated. The combination of halos of poles \mathbf{P}_u and zrot \mathbf{P}_u is an *elementary halo composite*. The symmetry group of this halo composite is 2.

The Wedge Change Corollary (Ref. 5, Subsection 3.O) indicates the conditions for which a symmetry higher than 2-symmetry occurs in halo composites. The Wedge Change Corollary is formulated from the viewpoint of light scattering from an individual crystal. In generalized form this corollary also applies to crystal ensembles.

Generalized Wedge Change Corollary

Assume that there are two congruent wedges A_1 and A_2 in an ensemble, not necessary on the same crystal. Assume the SVA to be satisfied. Let the halo that is due to A_1 have poles $\mathbf{P}_u = (a, b, c)$ and zrot $\mathbf{P}_u = (-a, -b, c)$. Ignore additional translation that may be

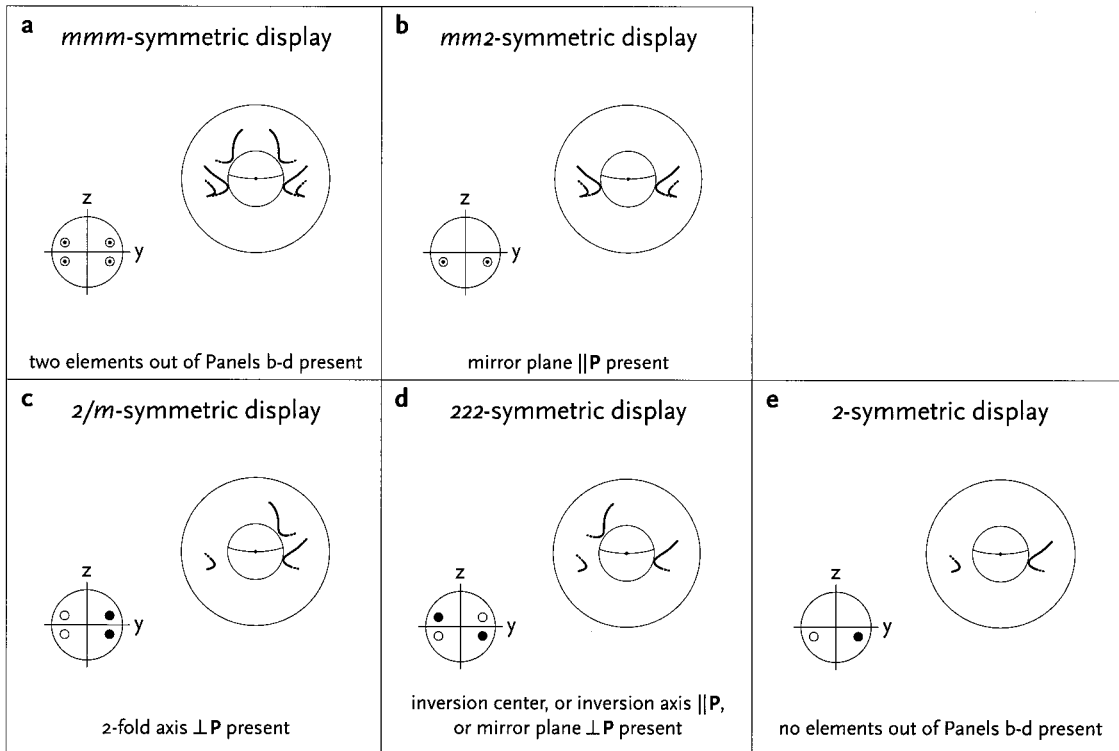


Fig. 1. The five halo symmetry groups. Each panel shows the pole diagram associated to a halo symmetry group, the resulting display of point halos, and a description of the crystal symmetry conditions that are required for generating these halo symmetries. \mathbf{P} is the crystal spin axis. According to the Crystal Orientation Corollary, only halo symmetry groups that result in L-R symmetric composites (mmm , $mm2$) can arise from crystals that are formed from the surrounding vapor. They are depicted in the upper row, which are panels a and b. The three halo symmetry groups that lack L-R symmetry ($2/m$, 222 , 2 -symmetric; panels c-e) are not expected to occur in natural circumstances. See Table 1 for more details. The depicted halos are for wedge angle 60° , refraction index 1.31, solar elevation 40° . The composites consist of the point halo with $\mathbf{P}_u = (1/4\sqrt{2}, 1/2\sqrt{3}, -1/4\sqrt{2}) \equiv B(30^\circ, 45^\circ)$, together with the halos from the induced poles according to the mmm , $mm2$, $2/m$, 222 , and 2 symmetry. These halos are the 22° equivalents of the 46° Parry infralateral and supralateral arcs. Solid circles in the pole diagrams refer to halo poles that are on the front hemisphere of the halo sphere; open circles, to halo poles on the rear hemisphere. In a $mm2$ -symmetric halo display that consist of halo composites from several wedges, the missing halos may be the upper arcs for a given halo-making wedge (like the situation in panel b), whereas for other halo-making wedges, the missing arcs may be the lower arcs instead. Similar arguments hold for $2/m$, 222 , and 2 -symmetric halo composites.

needed to map A_1 into A_2 . Then for fixed values of n and Σ

i. If at any moment A_1 can be transformed into A_2 by a rotation of \mathbf{P} about the zenith vector \mathbf{k} followed by a rotation of A_1 about \mathbf{P} , then the halos due to A_1 and A_2 are identical.

ii. If at any moment A_1 can be transformed into A_2 by a rotation of \mathbf{P} about \mathbf{k} followed by a rotation of A_1 of 180° perpendicular to \mathbf{P} and then possibly by a rotation of A_1 about \mathbf{P} , then the values of the halo poles due to A_2 are $(-a, -b, -c)$ and $(a, b, -c)$. The composite consisting of the union of all halos due to A_1 and A_2 is $2/m$ -symmetric.

iii. If at any moment A_1 can be transformed into A_2 by a rotation of \mathbf{P} about \mathbf{k} followed by a reflection of A_1 in a mirror plane parallel with \mathbf{P} , then the values of the halo poles due to A_2 are $(a, -b, c)$ and $(-a, b, c)$. That is, the halo composite due to A_2 and the halo composite due to A_1 are each other's L-R reflection with respect to the solar vertical. The composite consisting of the union of all halos due to A_1 and A_2 is $mm2$ -symmetric.

iv. If at any moment A_1 can be transformed into A_2 by a rotation of \mathbf{P} about \mathbf{k} followed by an inversion of A_1 and possibly by a rotation about \mathbf{P} , then the values of the halo poles due to A_2 are $(-a, b, -c)$ and $(a, -b, -c)$. The composite consisting of the union of all halos due to A_1 and A_2 is 222 -symmetric.

v. If two out of the conditions ii-iv satisfy in the ensemble, then the halo composite is mmm -symmetric.

Figure 1 shows the shapes of composites of point halos of the five possible halo symmetry groups, together with the arrangements of the poles on the halo sphere. The first and fourth columns of Table 1 give, for crystals with orientation preassigned in a mode allowed by the SVA, the link between symmetry of crystals and the symmetry group of the halo composites.

B. Wedge-, Orientation-, Crystal-, and Ensemble-Induced Halo Symmetry

The conditions of the Generalized Wedge Change Corollary can be satisfied in four different ways: from the symmetry of the individual wedges, from the

Table 1. Symmetry of Crystals and Symmetry in Halo Displays^a

Crystal Symmetry Condition		Point-Halo Symmetry Group			Great Circle Halo Symmetry Group		
		Preassn.	Polyh.	Crystal	Preassn	Polyh.	Crystal
1	None out of 2–5	2	2	<i>mm2</i>	2/ <i>m</i>	2/ <i>m</i>	<i>mmm</i>
2	Mirror plane inclined to P , or inversion axis inclined to P	2	<i>mm2</i>	<i>mm2</i>	2/ <i>m</i>	<i>mmm</i>	<i>mmm</i>
3	two-fold axis \perp P	2/ <i>m</i>	2/ <i>m</i>	<i>mmm</i>	2/ <i>m</i>	2/ <i>m</i>	<i>mmm</i>
4	Mirror plane \parallel P	<i>mm2</i>	<i>mm2</i>	<i>mm2</i>	<i>mmm</i>	<i>mmm</i>	<i>mmm</i>
5	Inversion center, or inversion axis \parallel P , or mirror plane \perp P	222	<i>mmm</i>	<i>mmm</i>	<i>mmm</i>	<i>mmm</i>	<i>mmm</i>

^a*Preassn.* refers to halos from polyhedrons (or crystals) whose orientation is preassigned in a mode allowed by the SVA. *Polyh.* refers to halos from congruent polyhedrons that preferentially orient from random initial conditions. *Crystal* refers to halos from an ensemble of preferentially oriented crystals that are formed from the surrounding vapor. If two crystal symmetry conditions are fulfilled, and if they generate nonidentical halo symmetry groups of symmetry higher than 2, then the display is *mmm*-symmetric. **P** is the crystal spin axis. The table assumes that the Gravity Organizing Principle (GOP) is satisfied.

wedge- or crystal orientations, from the crystal symmetry, and from the ensemble. We treat these cases subsequently.

Any wedge has the symmetry of the *mm2* point group: a mirror plane parallel to the bisector plane of the wedge, a second mirror plane perpendicular to the first one and to the edge of the wedge, and a twofold rotation axis in the intersection of these planes. An individual wedge is able to satisfy condition ii or iii. If this happens, then the halos from this wedge will bear the symmetry corresponding to ii or iii, irregardless of the symmetry of the halo-generating crystals. We call this halo symmetry *wedge induced*. In the case of wedge-induced symmetry, the halo poles are on the coordinate planes $x = 0$, $y = 0$, or $z = 0$ of the halo sphere. Conversely, if the poles have values $x = 0$, $y = 0$, or $z = 0$, then the halo symmetry is wedge induced. The occurrence of wedge-induced symmetry can obscure information about the (absence of) symmetry in the halo-generating crystals.

An example in which wedge-induced symmetry may occur is in halos from a crystal consisting of a scalene triangular basal face and three pyramidal faces that all three make the same angle with the basal face. This crystal has no symmetry element. However, if **P** is perpendicular to the basal face, then it is parallel to a mirror plane of each pair of faces of the crystal. Consequently, despite of lack of symmetry in the crystal, the halo display of this crystal is *mm2* symmetric. The poles \mathbf{P}_u of the halos are on the $x = 0$ plane or the $y = 0$ plane of the halo sphere.

Orientation-induced symmetry can happen as consequence of the SVA. An individual crystal or wedge may then satisfy one of conditions ii–iv of the Generalized Wedge Change Corollary with respect to its position after a 180° rotation about **P**. An example is a wedge that creates the 22° parhelion. A wedge has no center of symmetry, but if the spin axis **P** is parallel to its edge, then the wedge will assume after a while a position that is its 180° rotation about its edge. The wedge in its new position transforms to the wedge in its original position by an inversion through a center of symmetry. In this example, condition iv is satisfied in the time domain rather than at

any fixed moment. If one assumes the SVA to be satisfied statistically rather than physically, then condition iv is satisfied in space.

A second, more important, example is the fact that for great circle halos ($\psi = 90^\circ$), condition ii is always fulfilled by orientation induction. Consider a crystal at a certain moment and then the same crystal after its **P** has rotated by 180° about **k**. In the second situation, the crystal has also rotated by some angle about **P**. Then its original position can be obtained by a condition ii satisfying procedure: a 180° rotation perpendicular to **P** followed by a rotation about **P**. Because of $\psi = 90^\circ$, this procedure is always possible. This implies that great circle halo composites exhibit at least orientation-induced 2/*m*-symmetry. The only other symmetry group that is possible for great circle halo composites is the full *mmm*-symmetry (see Table 1).

Crystal-induced symmetry may arise if an entire crystal (or polyhedron) maps to itself by one of the symmetry operations described in conditions ii–iv of the Generalized Wedge Change Corollary. The halo composite is

- 2/*m*-symmetric if the crystal maps to itself by a twofold rotation about an axis perpendicular to **P**.
- *mm2*-symmetric if the crystal is its own mirror image across a plane parallel with **P**.
- 222-symmetric if the crystal maps to itself by an inversion, or by an inversion followed by a rotation about **P**. This includes reflection about a plane perpendicular to **P** and the operation of any rotatory-inversion axis parallel with **P**.
- *mmm*-symmetric if the crystal has two of the above properties.

Ensemble-induced symmetry arises if a crystal ensemble consists of two populations that are related via an operation satisfying the Generalized Wedge Change Corollary. A trivial example is an ensemble consisting of congruent crystals that are shaped like regular pyramids. If they were all oriented in the same way, with the pyramid axis vertical and the basal face down, then the ensemble satisfies only condition iii and the halo composite is *mm2*-

symmetric. However, if half the crystals are floating upside down (hence pyramidal axis vertical but basal face up), then condition ii (and iv) is satisfied by ensemble induction. Because of condition v, the halo composite is *mmm*-symmetric.

C. Crystal Orientations in Ensembles

We consider two situations that create ensemble-induced symmetry in halos. They are called here the *Polyhedron Orientation Theorem* and the *Crystal Orientation Theorem*. Both theorems assume that the Gravity Organizing Principle (GOP; see Section 1) is satisfied and that the orientations of the particles in the ensemble have evolved to stable final states.

The *Polyhedron Orientation Theorem* applies to floating polyhedrons that need not be formed from the surrounding vapor, but assumes random initial conditions when they became airborne. It applies, e.g., to a handful of crystals thrown into the air, or to artificially manufactured polyhedrons that are thrown into the air. The *Polyhedron Orientation Theorem* applies to a more generic situation than that of natural crystals formed from the surrounding vapor. Nevertheless, the *Polyhedron Orientation Theorem* considerably restricts the possibilities for formation of low-symmetric halo displays compared with the situation in which the orientation of crystals is preassigned in a mode allowed by the SVA. The consequences of the *Polyhedron Orientation Theorem* for halo formation are formulated in the *Polyhedron Orientation Corollary*.

The *Crystal Orientation Theorem* applies to floating crystals that are formed from the surrounding vapor. The *Crystal Orientation Theorem* can be considered to apply to all cases in which crystals are formed in planetary atmospheres. The *Crystal Orientation Theorem* restricts the possibilities for formation of low-symmetric halo displays even more than the *Polyhedron Orientation Theorem*. The consequences of the *Crystal Orientation Theorem* for halo formation are formulated in the *Crystal Orientation Corollary*. It should be emphasized that the *Polyhedron Orientation Corollary* as well as the *Crystal Orientation Corollary* apply to any kind of halo, instead of just to refraction halos.

As above, in the formulations that follow now, we ignore additional translations that may be needed to map one crystal shape into another.

Polyhedron Orientation Theorem

Let the elements of an ensemble of preferentially oriented congruent polyhedrons originate from random initial conditions when they became airborne. Let the polyhedrons be their own mirror image across some plane, or let the polyhedrons be their own inversion, or let the polyhedrons map to themselves by an *n*-fold rotatory-inversion axis. Then, in the ensemble, for each polyhedron A with spin axis \mathbf{P} fixed in it in a direction that is not necessary parallel to a symmetry axis of A, there exists a polyhedron B that is the mirror image of A across a plane that is $\|\mathbf{P}$ and where \mathbf{P} is the spin axis of B. The number of poly-

hedrons with an orientation and spin axis that correspond to that of polyhedron A and with the zenith angle of \mathbf{P} fixed at a given value ψ_o is equal to the number of polyhedrons with an orientation and spin axis that corresponds to that of polyhedron B and with the zenith angle of \mathbf{P} fixed at the same value ψ_o .

Justification of the Polyhedron Orientation Theorem

a. If a polyhedron satisfies one of the conditions of the *Polyhedron Orientation Theorem*, then there exists a rotation that transforms the polyhedron A into its mirror image B with respect to a plane $\|\mathbf{P}$.

Proof: A 180° rotation about an axis perpendicular to \mathbf{P} and to the rotatory-inversion axis (which includes the normal of a mirror plane), followed by a rotation about the rotatory-inversion axis, maps such a polyhedron into itself.

b. If the GOP is satisfied, then the flow conditions around a polyhedron A spinning in a plus direction about \mathbf{P} while \mathbf{P} has a fixed zenith angle and rotates in a plus direction about the zenith vector \mathbf{k} are equal to that of its mirror-image polyhedron B spinning in the minus direction about \mathbf{P} if \mathbf{P} has the same value for the zenith angle and rotates in a minus direction about \mathbf{k} . This implies that there is no mechanism to cause a preference for a polyhedron to end up in an orientation that corresponds to shape A instead of in an orientation that corresponds to shape B, and vice versa.

Polyhedron Orientation Corollary

Let the elements of an ensemble of preferentially oriented congruent polyhedrons originate from random initial conditions when they became airborne. Let the polyhedrons be their own mirror image across some plane, or let the polyhedrons be their own inversion, or let the polyhedrons map to themselves by an *n*-fold rotatory-inversion axis. Then, for the ensemble, the scattering cross sections for formation of a halo arc and its mirror image with respect to the solar vertical are equal.

Examples

1. Consider an ensemble of congruent regular hexagonal ice crystals, each having one basal face at one end and a pyramidal face instead of a basal face on the other end. In Tape's¹ face notation, the eight faces of the crystals are prism faces 3–8, basal face 2, and pyramidal face 14. Let a number of crystals to have assumed the Parry orientation with prism face 3 on top. Then, according to the *Polyhedron Orientation Theorem*, there will be an equal number of crystals in the ensemble that also have assumed the Parry orientation but now with prism face 5 on top. In accordance with the *Polyhedron Orientation Corollary*, the halo display from the ensemble of these two crystals will be L–R symmetric.

2. An orthorhombic disphenoid does not satisfy the conditions of the *Polyhedron Orientation Theorem*. An ensemble of congruent orthorhombic disphenoids will produce halos that are not L–R symmetric.

Crystal Orientation Theorem

Let an ensemble of preferentially oriented crystals be formed from the surrounding vapor. Then, in the ensemble, for each crystal A with spin axis \mathbf{P} fixed in it, there exists a crystal B that is the mirror image of A across a plane $\parallel \mathbf{P}$ and where \mathbf{P} is the spin axis of B. The number and the size distribution of crystals of shape and spin axis like A and with the zenith angle of \mathbf{P} fixed at a given value ψ_o are equal to the number and the size distribution of crystals of shape and spin axis like B with the zenith angle of \mathbf{P} fixed at the same value ψ_o .

Justification of the Crystal Orientation Theorem

a. Any crystallographic system allows for the formation of two crystals A and C that are each other's inversion.

b. A 180° rotation of crystal C about an axis perpendicular to \mathbf{P} transforms the crystal into a crystal B, which is the mirror image of crystal A across a plane $\parallel \mathbf{P}$.

Proof: This follows from the identity $\text{xrot}(-\mathbf{N}) = \text{xref } \mathbf{N}$.

c. If the GOP is satisfied, then the flow conditions around a crystal A spinning in a plus direction about \mathbf{P} while \mathbf{P} has a fixed zenith angle and rotates in a plus direction about the zenith vector \mathbf{k} are equal to that of its mirror-image crystal B spinning in the minus direction about \mathbf{P} if \mathbf{P} has the same value for the zenith angle and rotates in a minus direction about \mathbf{k} . This implies that there is no mechanism to cause preference for formation of a crystal that is shaped like crystal A and in an orientation corresponding to crystal A, instead of formation of a crystal that is shaped like crystal B and in an orientation that corresponds to crystal B, and vice versa.

Crystal Orientation Corollary

Let an ensemble of preferentially oriented crystals be formed from the surrounding vapor. Then, for this ensemble, the scattering cross sections for formation of a halo arc and its mirror image with respect to the solar vertical are equal.

Example

1. If an atmosphere allows for the formation of orthorhombic disphenoidal crystals, it allows with the same probability to orthorhombic disphenoidal crystals that are the mirror image across a plane $\parallel \mathbf{P}$. The ensemble of disphenoidal crystals will produce halos that are L-R symmetric. The same applies to, e.g., crystals shaped like asymmetric tetrahedra.

Consequences of the Crystal Orientation Corollary

1. Assume that the left and right components of a halo display from a homogeneous cloud of naturally formed crystals are not of equal brightness. Then the number of sunlit crystals in the line of sight of a given elevation is dependent on azimuth, or the light-

ing conditions of the crystals generating the two components of the halo are not equal.

2. Halo displays from crystals that are formed in an atmosphere are always L-R symmetric. Point halo displays may be either *mmm*-symmetric or *mm2*-symmetric. The latter requires the crystals to lack an inversion center, a rotatory-inversion axis $\parallel \mathbf{P}$, a mirror plane $\perp \mathbf{P}$, and a twofold axis $\perp \mathbf{P}$. Great circle halo displays are always *mmm*-symmetric.

3. Halo displays of 2, *222*, or *2/m*-symmetry are not expected to occur in nature.

The possibilities of halo symmetry for preassigned crystal orientation, according to the Polyhedral Orientation Corollary and according to the Crystal Orientation Corollary, are included in Table 1.

D. Additional Property

Definition. Let the faces f_1 and f_2 on a crystal form a halo-making wedge (f_1, f_2). If the full symmetry of the crystallographic system to which the crystal belongs allows for a transformation from f_1 to f_2 , then the wedge (f_1, f_2) is called *homoformic*; otherwise, the wedge (f_1, f_2) is called *heteroformic*.

Poles of Halos Resulting from Homoformic and Heteroformic Wedges

Let a crystal belong to a crystallographic system other than the cubic system. Let the crystal main axis be parallel to \mathbf{P} . Then

1. Halos poles resulting from homoformic wedges on the crystal are either on the equator of the halo sphere ($z = 0$) or on $x = 0$. The symmetry of all resulting halos is wedge induced.

2. Halos poles resulting from heteroformic wedges on the crystal are not on $z = 0$ or on $x = 0$.

Examples of homoformic wedges in ice crystals are those consisting of two prism faces (22° halos) or of two pyramidal faces (e.g., 18° or 35° halos). The wedges that make the 22° halos have both faces from the $\{1,0,-1,0\}$ form of the full hexagonal symmetry; the wedges that make the 18° and 35° halos have both faces from the $\{1,0,-1,1\}$ form. If ice is plate oriented, then the 22° and 35° halos poles are on $x = 0$. The 18° halos, which arise from pyramidal faces at different ends of the crystal, have their poles at $z = 0$.

Examples of heteroformic wedges in ice crystals are those consisting of one prism face and one pyramidal face (24° halos), or consisting of one prism face and one basal face (46° halos). If crystals are plate oriented, halo poles resulting from heteroformic wedges do not appear at $x = 0$ or $z = 0$. However, as the circumzenith arc demonstrates, they may appear at $y = 0$.

3. Crystal Reconstruction from Pole Diagrams: Method and Two Examples

A. Method

Assume that there is a halo display, and assume that the poles \mathbf{P}_u of the halos can be inferred (e.g., with the

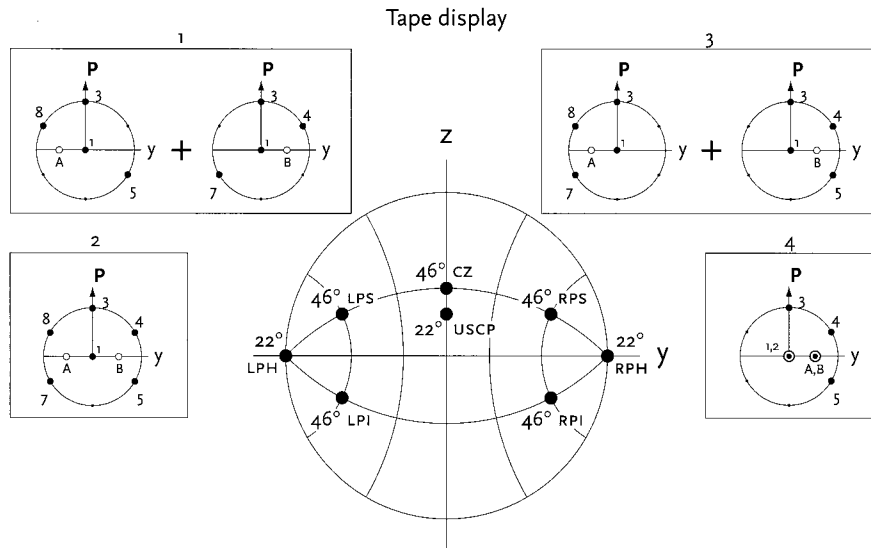


Fig. 2. Halo poles for point halos in the Tape display. The radius of the associated circular halo is indicated at each pole. On the $y = 0$ plane are the poles of the circumzenith arc (CZ) and the upper suncave Parry arc (USCP). The $(0, \pm 1, 0)$ poles are those of the left and the right parahelia (LPH and RPH). The remaining poles are those of the left and the right Parry supralateral arcs (LPS and RPS) and the left and the right Parry infralateral arcs (LPI and RPI). Around the halo sphere are four solutions to the minimum configuration of the halo-making crystals, as inferred from the occurrence of the halos (spin axis \mathbf{P} vertical; crystal main axis normal to the paper). Solid circles in the crystal diagrams refer to face normals pointing to the front hemisphere of the diagrams or that are parallel to the paper; open circles, to face normals pointing to the rear hemisphere. The face numbering is according to Tape's¹ system. The Tape display is on the cover of his book¹; a simulation of the display is on the back cover.

techniques of Ref. 5, Fig. 18) and that the angles α of the halo-making wedges are known. Then it is possible to construct minimum configurations for the halo-generating crystals by cutting and pasting the wedges together.

The method works as follows:

1. Define a coordinate system (x, y, z) with $z \parallel \mathbf{P}$ (\mathbf{P} is the spin vector). The sphere with radius unity is called the *face normal sphere*.

2. Select a halo pole \mathbf{P}_u . Determine on the halo sphere the angles θ_1, θ_2 between \mathbf{P}_u and the face normals $\mathbf{N}_1, \mathbf{N}_2$ of the halo-generating wedge.

3. Take $\theta_1 \neq 0, 180^\circ$. Then define the y plane of the face normal sphere as the plane $(\mathbf{P}, \mathbf{N}_1)$. Project the positions of \mathbf{N}_1 and \mathbf{N}_2 onto the face normal sphere. The colatitude and longitude of \mathbf{N}_1 are $(\theta_1, 0)$; that of \mathbf{N}_2 are (θ_2, δ) .

4. Select a second halo pole \mathbf{P}_u . Determine the angles θ_3 and θ_4 between \mathbf{P}_u and the face normals \mathbf{N}_3 and \mathbf{N}_4 of the halo-generating wedge.

5. Investigate whether θ_3 or θ_4 is equal to the previously found colatitudes θ_1 or θ_2 . Assume that such an equality is found; e.g., $\theta_3 = \theta_2$. Then take $\mathbf{N}_3 = \mathbf{N}_2$ and determine the position of \mathbf{N}_4 on the face normal sphere.

6. Proceed with the next halo pole.

This procedure is in fact a trial-and-error method. Several solutions are possible. The following should be kept in mind:

- If various solutions are found, a selection between them may be performed on the basis of the

argument that some solutions to the crystal configuration are expected to generate halos that are not observed.

- However, such consistency arguments are usually only supporting and not conclusive. See, e.g., the example in ice halos, in which Parry arcs are usually observed with no Parry supralateral arcs.

- There exists a risk that an unrealistic crystal configuration is constructed, being a combination of the same crystal in two orientation modes. This may happen if the colatitude θ of a face of a halo-generating wedge of the crystal in one orientation mode is identical with, or close to, the colatitude of a face of a congruent or almost-congruent wedge while the crystal is in the second orientation mode.

- Since the crystal faces may form wedges that produce no halos, or may form more than one wedge producing the same halo (e.g., because of the presence of a rotation symmetry axis), the reconstructed crystal configurations will usually have fewer faces than the actual crystals.

- Any crystal reconstruction method is more powerful for point halos and for low solar elevations. One reason for this is that in the reversed cases the halos from different poles are apt to be indistinguishable from one another. Second, for decreasing solar elevations, fewer halos tend to be empty. See Ref. 5, Figs. 36 and 42.

The strength and limitations of this cut-and-paste method are illustrated in the two examples that follow.

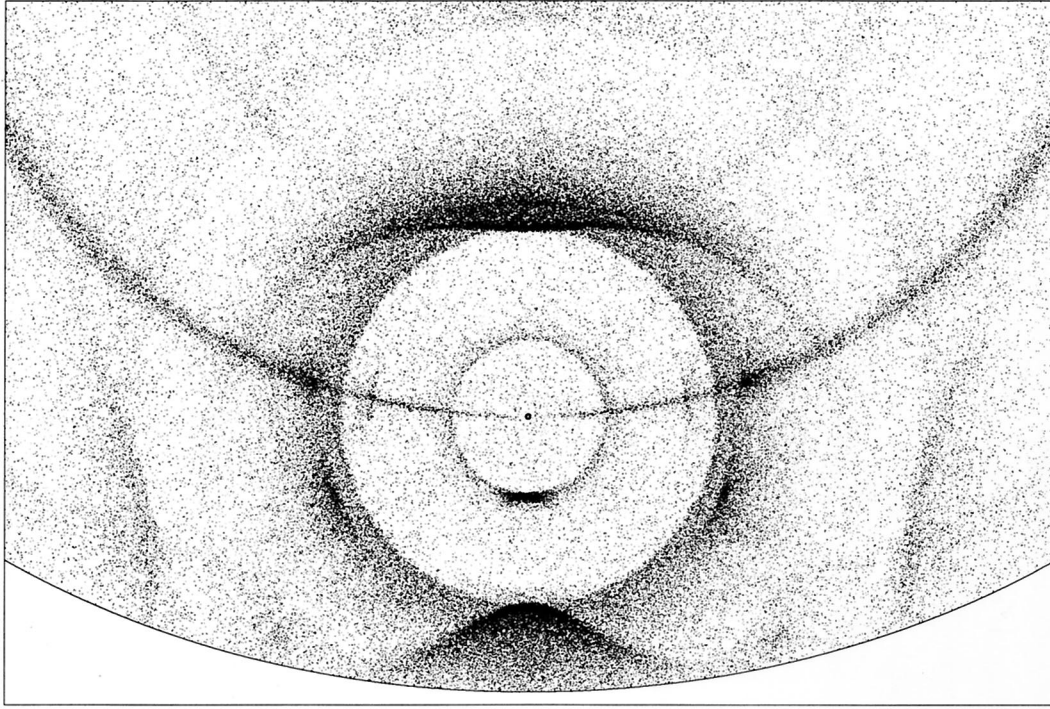


Fig. 3. Computer simulation of the Sturm display. The halos result from pyramidal ice crystals. The innermost circular halo is the 9° halo; the most prominent circular halo is the 22° halo. The mm_2 -symmetry of the display is apparent from the fact that some halo arcs (e.g., 9° , 24°) lack their counterparts on the other side of the parhelic circle. The simulation is shown in Fig. 10-19 of Ref. 1. A photograph of the display is shown in Ref. 1, Fig. 10-17. The pole diagram of the point halos in the display is shown in Fig. 4.

B. Example 1: Tape Display (2 January 1990)

This display was observed at U.S. Amundsen–Scott South Pole Station by Walter Tape. A picture is on the cover and in Fig. 2-11 of Tape's book¹; simulations are shown in Fig. 2-12 and on the back cover. We consider the point halos in this display. They have been successfully explained¹ from halo scattering by an ensemble of hexagonal prismatic crystals with basal ends, partly in plate orientation and partly in Parry orientation. Figure 2 (previous page) shows the poles of the point halos on the halo sphere. Visible from wedge angle 60° are the upper suncave Parry arc (USCP) and the left and right 22° parhelia (LPH, RPH). From 90° wedges, the circumzenith arc (CZ), and the left and the right Parry supralateral arcs (LPS, RPS) and the left and the right Parry infralateral arcs (LPI, RPI) are visible.

We now reanalyze the subset of the display consisting of point halos by our method. In the explanation of the reconstruction of crystal configurations that follows now, we denote the crystal faces according to Tape's¹ system: The basal faces are 1 and 2; the prism faces are 3–8, where in Parry orientation face 3 is on top. In finding the solutions depicted in Fig. 2, the starting point of all reconstructions is the CZ, whose pole relates face 3 to face 1. A compact notation for this is 1-(CZ)-3.

Solution 1, left (Fig. 2), follows from the string 1-(CZ)-3-(USCP)-5-(LPI)-1-(RPS)-8 and adds to this a peculiar face A by string 1-(LPH)-A (or equivalently, by string 1-(RPH)-A), in which face A gives the im-

pression of being part of a pyramidal cap. Solution 1, right, follows from similar strings following the halos on the other side of the solar vertical, i.e., 1-(CZ)-3-(USCP)-7-(RPI)-1-(LPS)-4 and 1-(RPH)-B. Solution 2 combines the two crystals of Solution 1 into one single crystal. From the Crystal Orientation Theorem it follows that no preference can be inferred from the halos between Solutions 1 and 2. Note that according to this theorem the two crystals of the dual-crystal Solution 1 should relate by a reflection across a mirror plane parallel to \mathbf{P} , as is indeed the case. Likewise, the single-crystal Solution 2 should bear a mirror plane parallel to \mathbf{P} , which is also true.

Solution 3 follows similarly from the strings 1-(CZ)-3-(USCP)-7-(RPI)-1-(RPS)-8 and 1-(CZ)-3-(USCP)-5-(RPI)-1-(LPS)-8, together with the two short strings leading to faces A and B. Combining the two crystals of Solution 3 into one single-crystal solution leads to either Solution 2 or Solution 4. Under the Crystal Orientation Theorem, Solution 4 is indeed allowed as an alternate single-crystal solution, as it also has a mirror plane parallel with \mathbf{P} . However, contrary to Solution 2, additional faces are required for completing its shape in a closed three-dimensional body.

As mentioned, there is no *a priori* preference to Solutions 1–4, although Solution 2 comes closest to a crystal with hexagonal symmetry. This single-crystal solution seems most attractive, although there is nothing more than common sense to support this preference. However, even Solution 2 is unre-

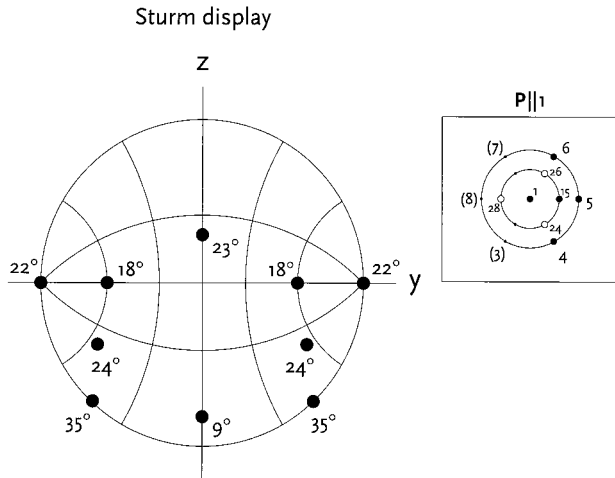


Fig. 4. Halo poles for point halos in the Sturm display (Fig. 3). The radius of the associated circular halo is indicated at each pole. The small diagram is a single-crystal solution to the minimum configuration of the halo-making crystals, as inferred from the occurrence of the halos (spin axis \mathbf{P} and crystal main axis normal to the paper). Solid circles in the crystal diagram refer to face normals pointing to the front hemisphere of the diagrams or that are parallel to the paper; open circles, to face normals pointing to the rear hemisphere. The face numbering is according to Tape's¹ system. Faces in brackets cannot be inferred from the display. The Sturm halo is shown in Fig. 10-17 of Tape's book.¹

alistic, as it actually invokes a pseudopyramidal crystal by combining Parry- and plate-oriented crystals by means of the CZ, which both orientations are capable of generating. The real solution is of course a proper decomposition of the single-crystal solutions into two crystals such that it removes the crystallographic impossible faces A and B from the Parry-oriented crystal. These faces A and B then become faces 3 and 5 from the second population, which is a plate-oriented crystal.

This example illustrates that crystals may indeed be reconstructed, but often only partially. Some faces may be missing. Also, the solutions are often not unique, whereas in this example readily unrealistic crystals are invoked by combination of halos from different orientation modes. It should be acknowledged, however, that this problem holds for computer simulations as well.

C. Example 2: Sturm Display (11 July 1987)

The Sturm halo was observed by Klaus Sturm on the German Georg von Neumayer station in the Antarctic. A picture is shown in Ref. 1, Fig. 10-17; a computer simulation is shown in Fig. 10-19 of Ref. 1 and reproduced here as Fig. 3. The halo display shows point halos associated to the 9°, 18°, 22°, 23°, 24°, and 35° halos. The display has been successfully interpreted from plate-oriented prismatic ice crystals with basal as well as pyramidal faces at the ends.¹ In accordance with the $mm2$ -symmetry of the display, the explaining crystals were thought to have developed the pyramidal faces at one end only, which is the downward end.

Figure 4 shows the halo poles of the Sturm display, together with a single-crystal solution to the reconstruction of the minimum configuration of a crystal from the halo-making wedges. The minimum configuration of the crystal was constructed under the assumption that all halo-making wedge angles were precisely known. The configuration can be found from two strings. The first one is 1-(23°)-28-(24°)-4-(22°)-6-(24°)-28-(35°)-26-(18°)-15-(18°)-24; the second one is 28-(9°)-5. The notation in both strings is such that the halo angles are in brackets; the face numbers are not. No halos are repetitively generated in this scheme. Because left and right 18° halos require a different wedge, this halo appears twice in the strings. The same is true for the 24° halos.

The crystal reproduced in Fig. 4 makes all the halos shown in the Sturm picture. Hence this crystal is sufficient to explain all observed features. It is tempting to apply a sixfold rotation symmetry operation to this crystal, which would transform the minimum-configuration crystal into a more realistic one, but there exists no empirical justification for this addition. Note that even if all wedges in the resulting sixfold symmetric crystal made a halo (including, e.g., the $\alpha = 120^\circ$ wedges), the manifestation of this crystal symmetry would remain hidden as long as the sixfold axis is parallel with the spin axis \mathbf{P} . If the crystal assumed another orientation, e.g., the Parry orientation as in the previous example, then the existence of more faces could be inferred from the display. This highlights a main limitation of any reconstruction of crystals from the appearance of halos. The other limitation is, as in the previous example, that it usually remains possible to express the solution in terms of two or more crystals, whose union is equal to the depicted crystal, and that there exists no way to decide what the real situation is. And again, this problem is a general one in any reconstruction method of halo-generating crystals, including Monte Carlo methods.

4. Titan Halos

A. Methane Halos and Ethane Halos

Within the current standard models of the Titan atmosphere⁴ there may be room for the presence of crystals of methane (CH_4) and perhaps of ethane (C_2H_6). Crystals of these compounds are transparent. If the sizes of the Titan crystals are larger than $\approx 20 \mu\text{m}$ and if the crystals are directly lit by the Sun, halos will appear in the Titan sky. Then there exists a possibility that the Huygens probe will detect these halos during a certain stage of its descent through the Titan atmosphere on 14 January 2005. The solar elevation at the descent is $40^\circ \pm 10^\circ$ (Ref. 4), and this number remained unchanged after the reschedule in 2001 of the Huygens mission.⁶ Figure 5 shows the shapes of mmm -symmetric point-halo composites for solar elevation 40° . In combination with the pole diagram (Fig. 6) of potential Titan halos of methane

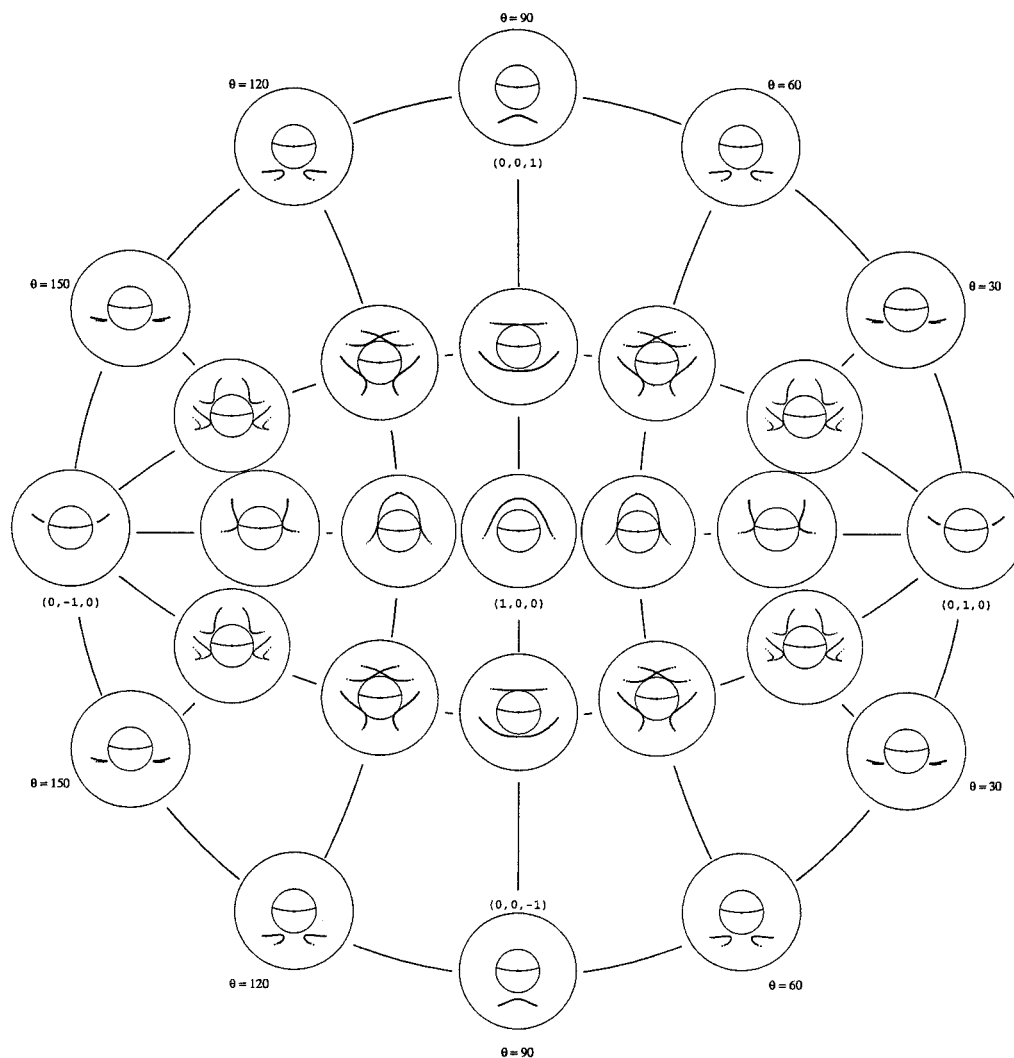


Fig. 5. Atlas for mmm -symmetric point-halo composites for solar elevation 40° . The wedge angle α is 60° ; refraction index is $n = 1.31$. Because the shapes of the halos are only weakly dependent on α and n , the atlas gives a fair impression how point halos associated to a certain halo pole are approximately shaped. The approximate shapes of Titan refraction halos that may be detected during the descent of the Huygens probe in Jan 2005 can be found by looking at the spots where the Titan halo poles (Fig. 6) appear. The coordinate θ indicates the Bravais colatitudes on the halo sphere.

or ethane, discussed below, it visualizes how point-halo displays arising from Titan crystals could be approximately shaped.

Methane [mp 91K, bp 109K (Ref. 7)] belongs to the cubic system; the estimated index of refraction at the melting point is 1.32.⁸ Likely simple crystal shapes are cubes, octahedrons, and square pyramids or, more generally, crystallographic combinations of a cube and an octahedron. Halo-making wedge angles α in these combinations are 54.7° (one octahedral face and one cubic face), 70.5° (two octahedral faces), and 90° (two cubic faces). These wedge angles correspond to halo angles of 20° , 29° , and 48° , respectively. Apart from random orientation, a plausible orientation mode for these crystals is one with the crystallographic main axis vertical (i.e., a cubic face horizontal). This orientation leads for all wedges to point halos with poles that are on the $y = 0$ plane, which are referred to as Parroid arcs⁹ because of the

similarity in properties with the ice-crystal Parry arcs. A comparison of Fig. 6 with the pole diagram of the 22° and 46° ice crystal halos (Ref. 5, Figs. 55 and 59) indicates a great similarity in shapes between the 20° methane Parroid arcs and the ice sun-cave Parry arcs, between the 29° methane Parroid arcs and the ice sunvex Parry arcs, and between the 48° methane Parroid arcs and the 46° ice circumzenith/horizon arcs. The formation of the methane Parroid arcs on Titan can occur from methane crystals of the simplest shape, i.e., square pyramids (20° and 29° halos) and cubes (48° halos).

In addition to the set of methane Parroid arcs, Fig. 6 indicate 48° methane parhelia [$\mathbf{P}_u = (0, \pm 1, 0)$], 29° methane halos with poles on the $z = 0$ plane and 20° methane halos with poles that are not on a coordinate plane of the halo sphere. The simplest crystal shape to make the 48° methane parhelia is a cube. The 29° halos at $z = 0$ requires an octahedron. The forma-

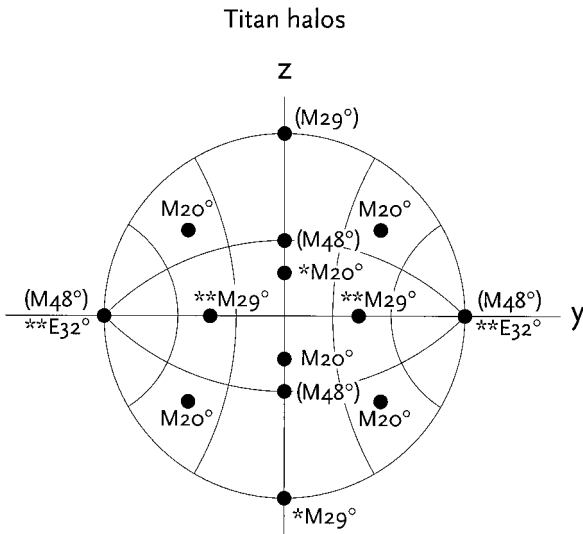


Fig. 6. Poles of Titan halos resulting from truncated octahedrons of methane (M) and from hexagonal crystals of ethane (E) with basal faces. The truncations apply to all vertices of the octahedrons. It is assumed that the methane and ethane crystal main axes are vertically oriented. Halos that are empty for solar elevation 40° are in brackets. However, for these halo angles, circular halos (not depictable in the pole diagrams) are always possible if the crystal orient randomly. The M 48° halos are due to two cubic faces, the M 29° halos to two octahedral faces, and the M 20° halos to one cubic and one octahedral face. Halos that are within the reach of the Huygens imagers are marked with *. These are the upper 20° methane Parroid arc and the lower 29° methane Parroid arc. The 32° ethane parhelia and the 29° methane halos from poles with $z = 0$, marked with **, are out of reach of the imagers, but their subhorizon counterparts (viz. the 32° ethane subparhelia and two halos that are shaped as the reflections of the two 29° halos in question at a horizontal mirror plane) are within reach. Figure 5 visualizes how an *mmm*-symmetric point halo display associated to a certain halo pole is approximately shaped. Figures 7–10 give a Monte Carlo simulation of a Titan halo display.

tion of the 20° halos outside the coordinate planes requires a more complicated combination of a cube and octahedron than a square pyramid, namely, octahedrons with truncations at the horizontal vertices so that vertical cubic faces are present. Intuitively the formation of such truncated crystals seems much less likely than that of square pyramids or that of octahedrons truncated at the upper or lower vertices. If that conjecture is correct, then the four 20° halos with poles off the coordinate planes (Fig. 6) can effectively be ruled out as Titan halo candidates.

Ethane [mp 90K, bp 185K (Ref. 7)] belongs, as does ice, to the hexagonal system (Refs. 7 and 10; see however Ref. 11). Therefore the crystal shapes and orientation modes of floating ethane crystals are probably similar to those of terrestrial ice. The estimated⁸ refractive index of solid ethane is 1.44¹⁰; the crystallographic axial ratio c/a is 1.84.¹⁰ The halo-making wedge angle in a hexagonal ethane prism ($\alpha = 60^\circ$) generates 32° halos, being the analogs to the 22° ice crystal halos. Randomly oriented ethane would result in a circular 32° halo, plate-oriented ethane crystals to 32° parhelia. For solar elevation

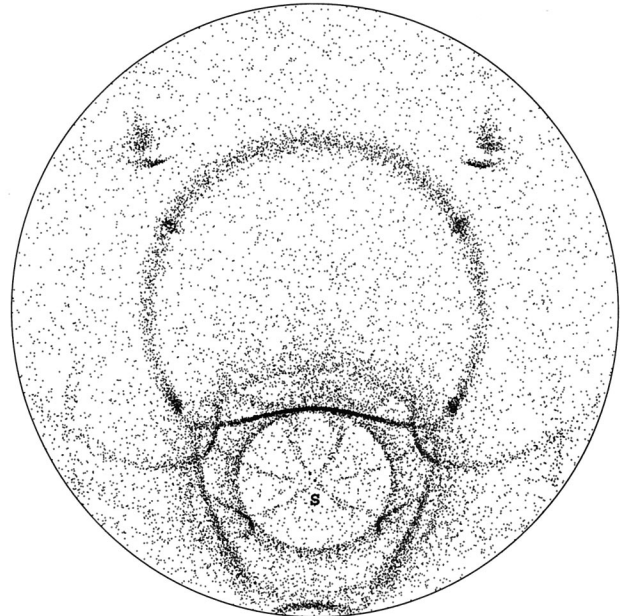


Fig. 7. Halo display that may occur in the Titan atmosphere during the decent of the Huygens probe. In this Monte Carlo ray-tracing simulation, there are four populations of methane crystals: square pyramids with cubic face up and with cubic face down, randomly oriented equidimensional cube-octahedrons with all vertices truncated, and equidimensional cube-octahedrons with the fourfold rotation symmetry axis vertical and all vertices truncated. Additionally, there are two ethane crystal populations: plate oriented and randomly oriented hexagonal crystals with basal ends. The standard deviation of the tilts of axes of the preferentially oriented crystals is 1° . The figure is uplooking with a field of view of 180° : The zenith is in the center, and the circle that surrounds the simulation is the horizon. The symbol S marks the position of the Sun, which is at 40° elevation. The prominent circular halo is the 20° methane circular halo; the three other possible circular halos are barely visible. Another choice for the populations or for the crystal parameters would result in different relative intensities of the various halos in the display. Fig. 10 is a legend to the refraction halos. The three above-horizon regions that are in the fields of view of the Huygens imagers consist of a 6° wide vertical band through the Sun extending from 15° till 65° above the horizon; a similar vertical band straight opposite to the Sun; and the entire region between the horizon and a height of 6° .

40° , these 32° parhelia would appear at 55° azimuthal distance from the Sun. Parry-oriented ethane would give rise to Parroid arcs that are similar to the Parry arcs in ice. Great circle 32° ethane halos from column orientation would be analogous to the upper or lower tangent arcs in ice. As the index of refraction of ethane exceeds $\sqrt{2}$, the analogs of the 46° ice halos ($\alpha = 90^\circ$) would not appear from ethane. The two ethane halos poles due to plate (column) orientation are included in Fig. 6; those from the (more improbable) Parry orientation are not.

Like ice, ethane crystals may develop pyramidal faces; such crystals would give rise to 11° , 27° , 25° , 36° , 35° , and 50° halos. They are the analogs of the 9° , 18° , 20° , 23° , 24° , and 35° ice halos, in that order.

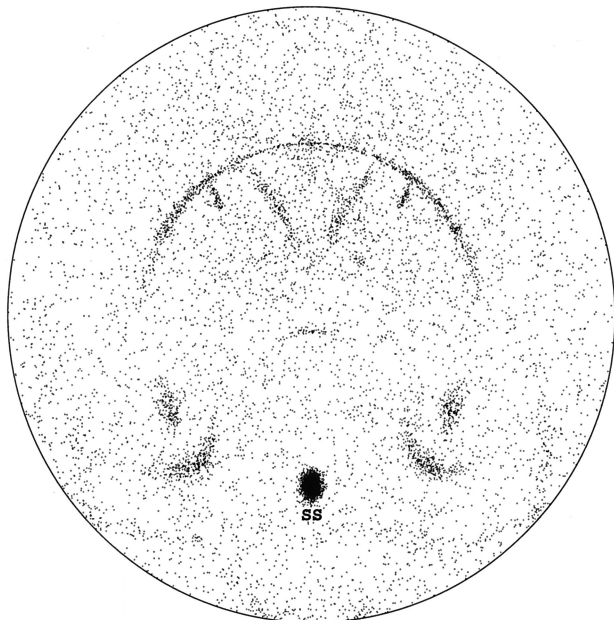


Fig. 8. Halo display that may occur in the Titan atmosphere. As in Fig. 7, but now downlooking: The nadir is in the center, and the circle that surrounds the simulation is the horizon. The symbol SS marks the position of subsun, which is the reflected image of the Sun at horizontal crystal faces. Hence the subsun is directly below the Sun and is as far below the horizon as the Sun is above. With exception of a circular region of 6.5° radius centered at the nadir, the entire subhorizon sky can be photographed by the Huygens probe.

Given the extreme rarity of halos resulting from pyramidal ice crystals on Earth, it seems highly improbable that the Huygens probe would happen to detect their ethane counterparts. A casual look at Fig. 5 in combination with the pole diagrams published in Ref. 5 (Figs. 52–59) tells how *mmm*-symmetric displays of these arcs would be approximately shaped.

In light of the complexity of the chemistry of the Titan atmosphere, there may be room for halo formation from crystalline compounds whose compositions have yet to be guessed. If such a surprise would happen, analysis of these halos as outlined in the previous paragraph may provide a clue to the nature of such crystals.

B. Huygens Prospects for Halo Detection

The prospects for detection of refraction halos during the Huygens descent are not in all aspects optimal. First, all methane 48° halos of Fig. 6 are empty for solar elevation 40° , which implies that no 48° point halos from methane can be generated at this solar elevation. Second, although the 32° ethane parhelia, the 29° methane halos from $z = 0$ poles, and the four 20° methane halos from the poles off the coordinate planes are potentially within the reach of the Huygens solar aureole (SA) imager, no pictures of these halos will be obtained. The reason for this is that these halos appear on either sides of the solar vertical, whereas the SA imager, having a horizontal

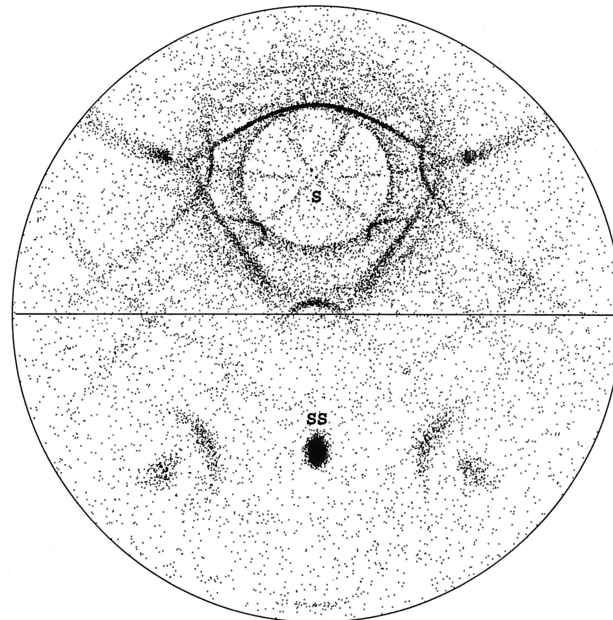


Fig. 9. Halo display that may occur in the Titan atmosphere. As in Fig. 7, but now facing to the point at the horizon straight below the Sun. The horizontal line is the horizon. The symbol S marks the position of the sun; the symbol SS marks the position of the subsun. The bright subhorizon halos emerge from light paths refraction–reflection–refraction, where the reflecting face is a horizontally oriented crystal face. The two subhorizon spots are the 32° ethane subparhelia, which appears as the reflected images of the 32° ethane parhelia from a horizontal mirror plane. The two other subhorizon arcs appear as the reflected images of the two 29° methane halos from poles with $z = 0$. Contrary to their above-horizon counterparts, they may arise from crystals as simple as square pyramids (with cubic face down).

field of view of only 6° , is scheduled to take only sunward and antisunward pictures.¹² Similarly, the lower 20° methane Parroid arc would be escape detection, because for solar elevation 40° this halo consists of two disconnected segments and has no part that is straight below the Sun. Third, none of the Huygens imagers cover heights above the horizon between 6° and 15° or heights exceeding 65° , implying for solar elevation 40° an observational gap in scattering angle between 25° and 34° . This rules out detection of the 29° methane or 32° ethane circular halo, for that solar elevation.

Of the detectable halos, the 48° methane circular halo would be in the field of view of the side-looking imager (SLI), which covers heights between -45° and $+6^\circ$. However, only the lower part of the halo would show up in the SLI images. The lower 29° methane Parroid arc is also in the field of view of the SLI, as this halo arc stays 8° clear from its associated circular halo for solar elevation 40° . Because the top of this arc would be less than 4° above the horizon, the entire arc may be photographed by the SLI. Furthermore, the upper 20° methane Parroid arc and its associated circular halo are in the field of view of the sunward images of the SA, as the SA imager cover heights between 15° and 65° (hence scattering angles up to

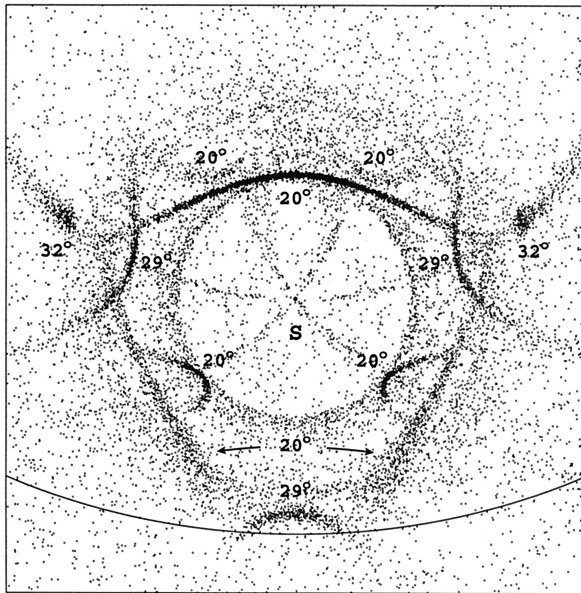


Fig. 10. Key to the refraction halos in Figs. 7–9. The radius of the circular halos that are associated with the various refraction halos are indicated. Halo angles printed in the solar vertical refer to Parroid arcs (poles on the $y = 0$ plane in the pole diagram, Fig. 6). The lower 20° methane Parroid arc consists of two disconnected halo arcs for this solar elevation. Halo angles printed near the parhelic circle (which is the solar almucantar) refer to halos from $z = 0$ poles. These include the 32° ethane parhelic. The remaining refraction halos are from the poles that are not on a coordinate plane of the halo sphere. The symbol S marks the position of the Sun.

25°). However, because of the narrow horizontal field of view of the SA, only portions of the halos that are straight above or below the Sun may be captured.

An interesting aspect of the SA imager is its capability to detect polarization. This capability enhances the possibilities for halo detection. Since halo light is polarized even for isotropic halogenerating crystals (polarization in the plane of scattering and degrees of polarization increasing from 1% to 5% for halo angles increasing from 10° to 25°), the presence of a 20° methane Parroid arc or a 20° methane circular halo may be apparent from a polarization anomaly. It is worthwhile to mention that if the SA imager would happen to be directed to a halo resulting from anisotropic crystals of some unanticipated compound, the existence of the halo birefringence peak in polarization may provide a truly sensitive means for halo detection.^{9,13}

It is quite possible that the solar elevation at the Huygens descent will end up in a value that differs more than 4° from its nominal 40° value or, more precisely formulated, that the solar elevation as viewed from Huygens when it crosses the heights where halo appearance may occur differs more than 4° from 40° . If this happens, then the SA is capable of detecting a 29° methane circular halo and perhaps a 32° ethane circular halo.

The conclusion of the foregoing is that among the

potential Titan refraction halos, the 20° methane circular halo, the upper 20° and the lower 29° methane Parroid arcs, and the 48° methane circular halo are definitely detectable by Huygens. The 29° methane circular halo still has a good chance to be in the field of view of the SA, but the prospects for the 32° ethane circular halo detection seem less favorable. The point halos associated with the remaining poles depicted in Fig. 6 are not detectable by Huygens.

In addition to the refraction halos discussed above, there exists a possibility of formation of Titan halos from ray paths that include internal reflections at the crystal faces. This type of halo is not restricted to small scattering angles. Among the terrestrial examples of such halos are the parhelic circle, and subhorizon halos such as the subsun or the subparhelia, of which the subsun is even more common than the refraction halos. A Titan methane or ethane parhelic circle may be detected in the antisunward images of the SA; subhorizon halos, including a methane or ethane subsun or subparhelic circle, a potential ethane 32° subparhelic, and two subhorizon methane halos that appear as a reflection of the two 29° halos with poles at $z = 0$, may be detected by the downlooking imagers. Figures 7–9 show a full Monte Carlo ray-tracing simulation of point halos and circular halos that may occur on Titan; Fig. 10 indicates the relation of the refraction halos of those simulations with the halo poles of Fig. 6.

The computer simulations in this article were provided by Walter Tape.

References

1. W. Tape, *Atmospheric Halos*, Vol. 64 of the Antarctic Research Series (American Geophysical Union, Washington, D.C., 1994).
2. M. Pekkola, M. Riikonen, J. Moilanen, and J. Ruuskanen, "Halo arcs from airborne, pyramidal ice crystals falling with their c axes in vertical orientation," *Appl. Opt.* **37**, 1435–1440 (1998).
3. M. Riikonen, M. Salinpää, L. Vira, D. Sullivan, J. Moilanen, and I. Luukonen, "Halo observations provide evidence of airborne cubic ice in the Earth's atmosphere," *Appl. Opt.* **39**, 6080–6085 (2000).
4. J.-P. Lebreton, ed., "Huygens, science payload and mission," ESA SP-1177 (European Space Agency Publication Division, ESTEC, Noordwijk, The Netherlands, 1997).
5. W. Tape, and G. P. Können, "A general setting for halo theory," *Appl. Opt.* **38**, 1552–1625 (1999).
6. J.-P. Lebreton, European Space Agency/ESTEC, Noordwijk, The Netherlands (personal communication, 2001).
7. R. C. Weast, ed., *CRC Handbook of Chemistry and Physics*, 62nd ed. (CRC Press, Boca Raton, Fla., 1981).
8. E. Whalley and G. E. McLaurin, "Refraction halos in the solar system. I. Halos from cubic crystals that may occur in atmospheres in the solar system," *J. Opt. Soc. Am. A* **1**, 1166–1170 (1984).
9. G. P. Können, "Identification of odd-radius halo arcs and of $44^\circ/46^\circ$ parhelia by their inner edge polarization," *Appl. Opt.* **37**, 1450–1456 (1998).
10. H. Mark and E. Pohland, "Über die Gitterstruktur des Äthans und des Diborans," *Z. Kristallogr.* **62**, 103–112 (1925).

11. G. J. H. van Nes and A. Vos, "Single-crystal structures and electron density distributions of ethane, ethylene and acetylene," *Acta Crystallogr. Sect. B* **34**, 1947–1956 (1978).
12. M. G. Tomasko, L. H. Doose, P. H. Smith, R. A. West, L. A. Solderblom, M. Combes, B. Bézard, A. Coustenis, C. deBergh, E. Lellouch, J. Rosenqvist, O. Saint-Pé, B. Schmitt, H. U. Keller, N. Thomas, and F. Gliem, "The descent imager/spectral radiometer (DISR) aboard Huygens," in *Huygens, Science Payload and Mission*, J.-P. Lebreton, ed., ESA SP-1177 (European Space Agency, Publication Division, ESTEC, Noordwijk, The Netherlands, 1997), pp. 109–138.
13. G. P. Können, A. A. Schoenmaker, and J. Tinbergen, "A polarimetric search for ice crystals in the upper atmosphere of Venus," *Icarus* **102**, 62–75 (1993).